Supporting Information

Ultrasound-Induced Piezoionic Hydrogel with Antibacterial and Antioxidant Properties for Promoting Infected Diabetic Wound Healing

Chunhua Huang[a,b,1], Xingxing Shi[a,b,1], Binying Peng[c,1], Jiapeng Song[a,b], Hanwen Huang[a,b], Bingna Zheng[a,b], Youchen Tang[a,b,], Zhaopeng Cai[a,b,]*, Peng Wang[a,b,]**

[a] *The Eighth Affiliated Hospital, Sun Yat-sen University, Shenzhen 518033, PR China*

[b] *Guangdong Provincial Clinical Research Center for Orthopedic Diseases, The Eighth Affiliated Hospital, Sun Yat-sen University, No. 3025 Shennan Road, Shenzhen, 518033, PR China.*

[c] *The Sixth Affiliated Hospital, Sun Yat-sen University, Guangzhou 510655, PR China*

* Corresponding authors.

E-mail addresses: tangych7@mail.sysu.edu.cn (Y. Tang), caizhp3@mail.sysu.edu.cn (Z. Cai), wangp57@mail.sysu.edu.cn (P. Wang).

[1] These authors contributed equally to this work.

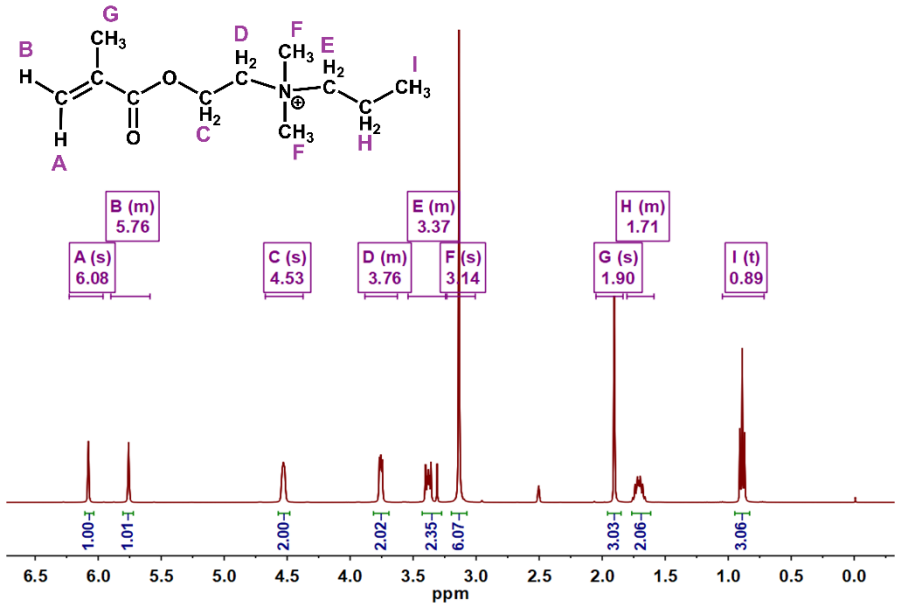

Fig. S1 ^{1}H NMR spectrum of DPAB.

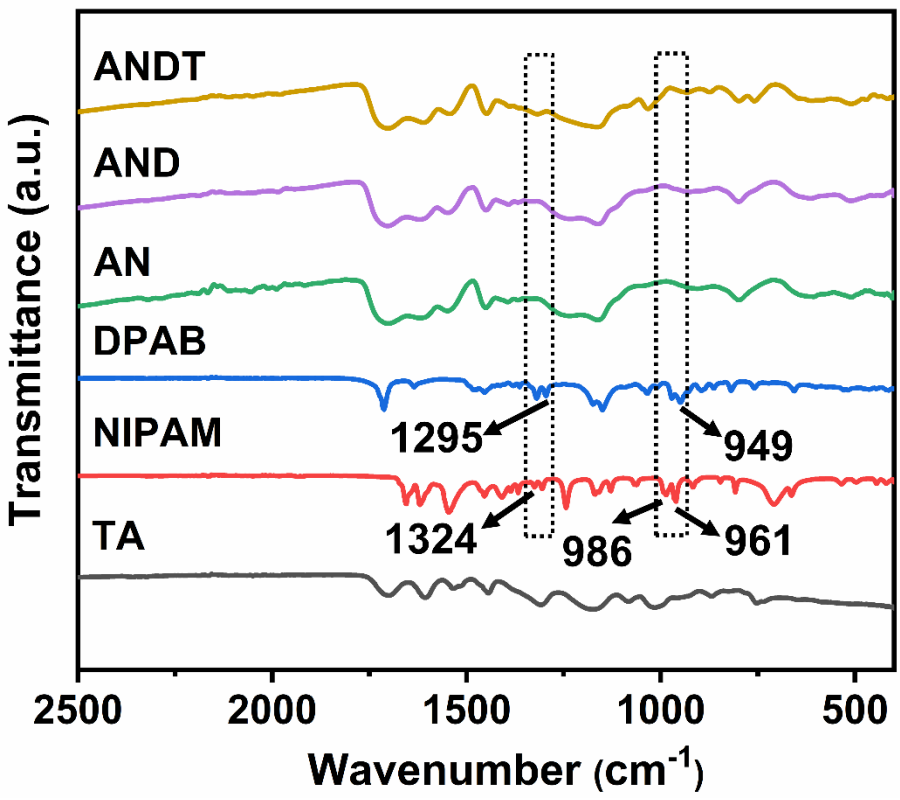

Fig. S2 FT-IR spectra of TA, NIPAM, DPAB, AN, AND, and ANDT.

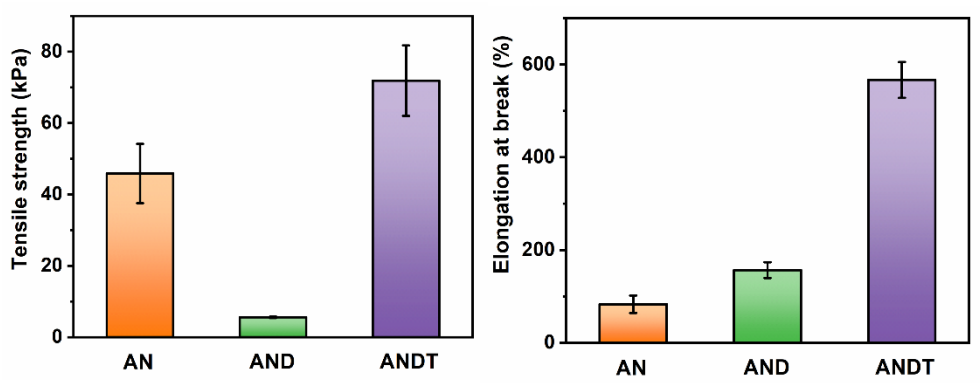

Fig. S3 (a) Tensile strength and (b) elongation at break of AN, AND, and ANDT hydrogels. The error bars show a standard deviation, $n = 3$.

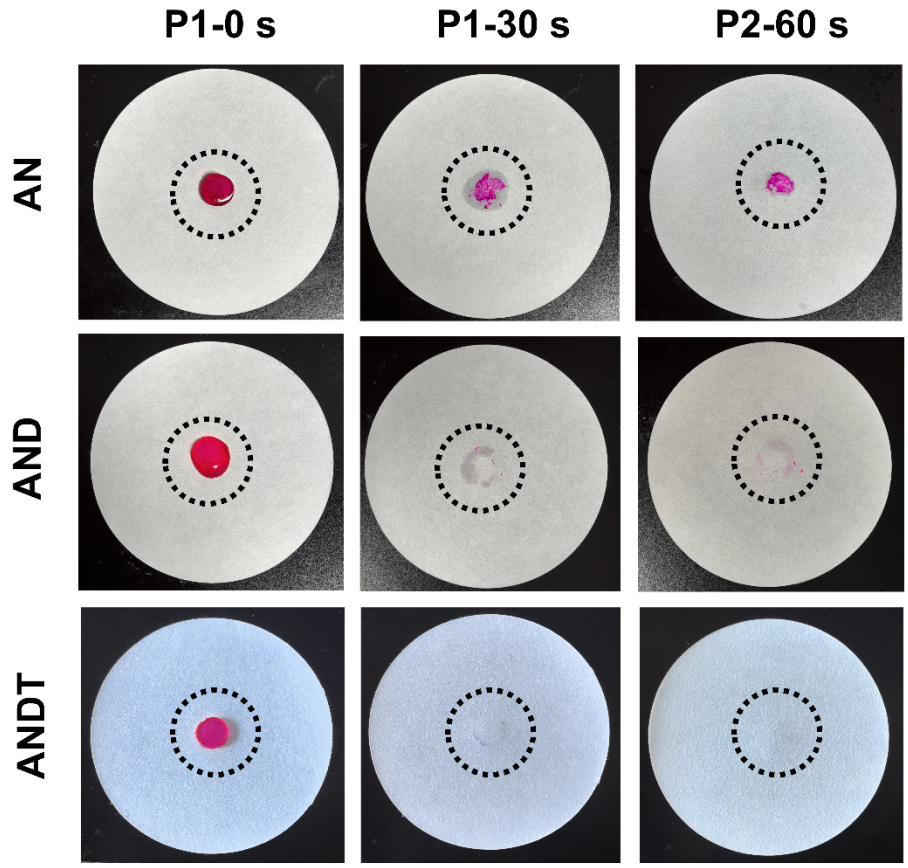

Fig. S4 The anti-reflux performances of AN, AND, and ANDT hydrogels. P1-0 s: hydrogel samples were placed directly on the first filter paper; P1-30 s: hydrogel samples were placed on the first filter paper for 30 s and then were removed; P2-60 s: hydrogel samples were placed on the second filter paper for 60 s and then were removed. For easy observation, the hydrogels were saturated with rhodamine B solution.

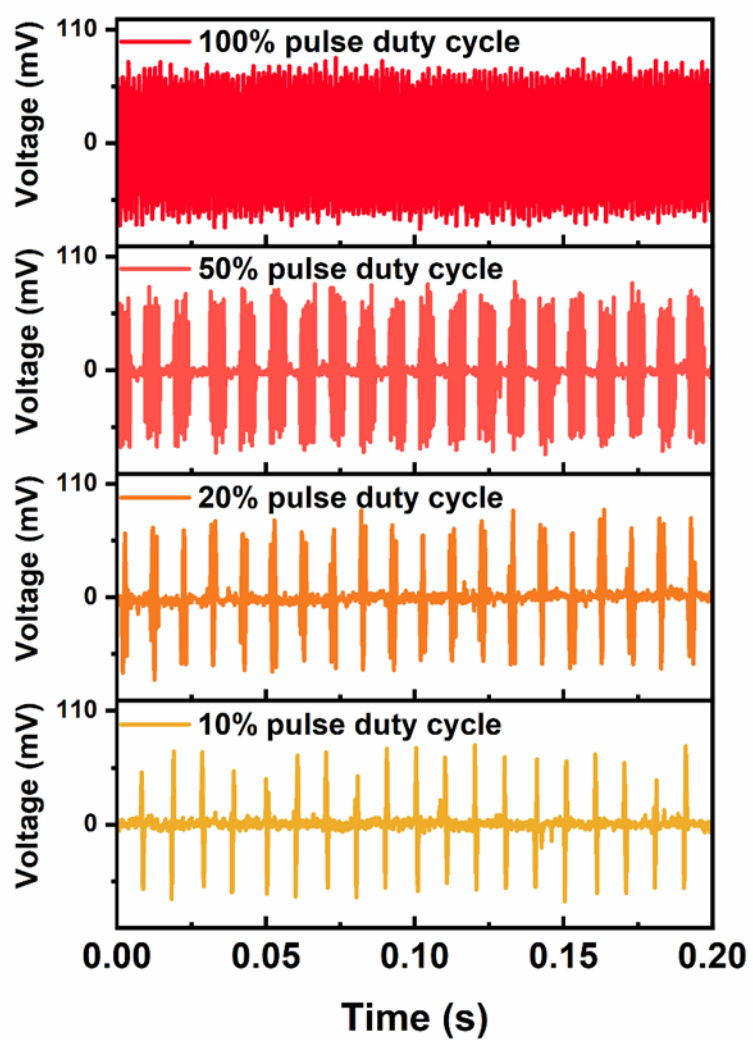

Fig. S5 The output voltages of ANDT hydrogel under 0.5 W/cm^2 with different pulse duty cycles.

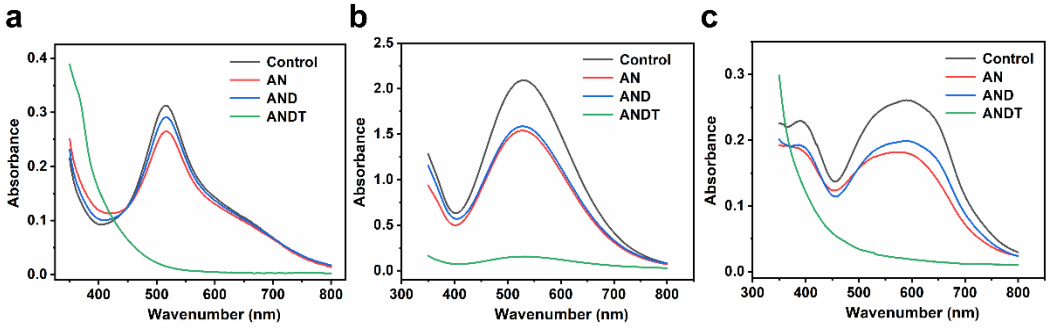

Fig. S6 Absorbance curves of control, AN, AND, and ANDT groups for (a) DPPH, (b) •OH, and (c) O_2^{-}• scavenging assays.

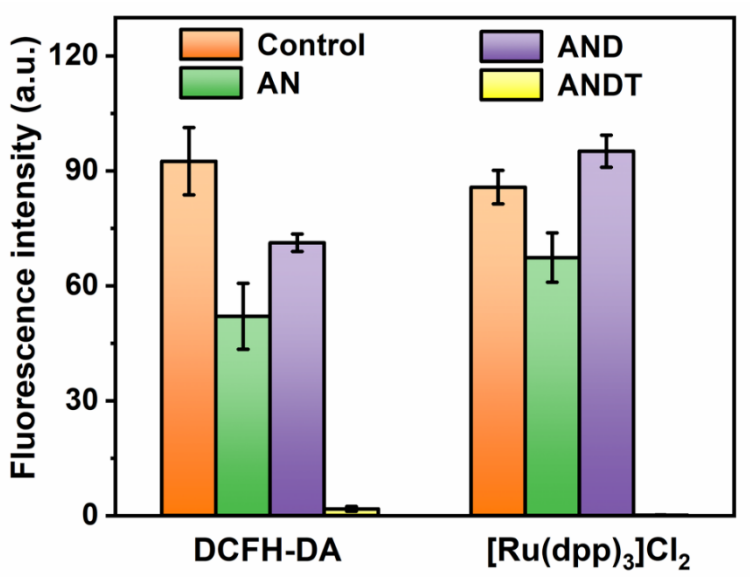

Fig. S7 Quantitative assay of fluorescence intensity of the DCFH-DA probe and $[Ru(dpp)_3]Cl_2$ indicator in L929 fibroblasts.

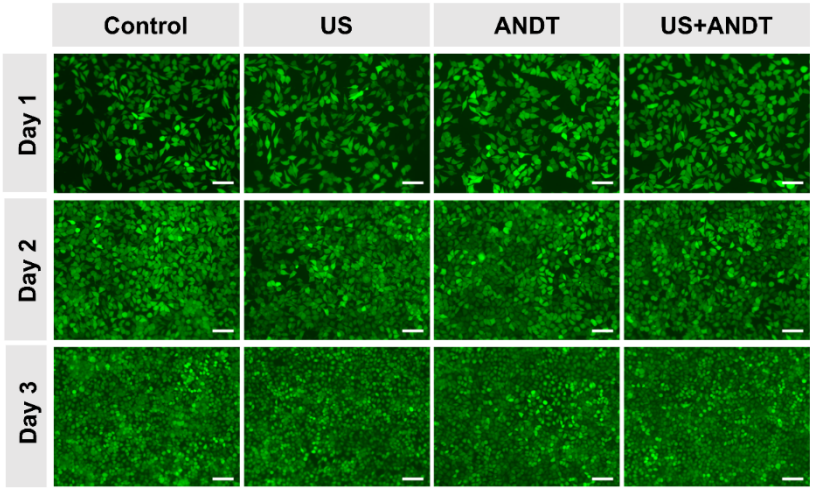

Fig. S8 Live/dead staining of L929 fibroblasts (scale bars = 100 μm).

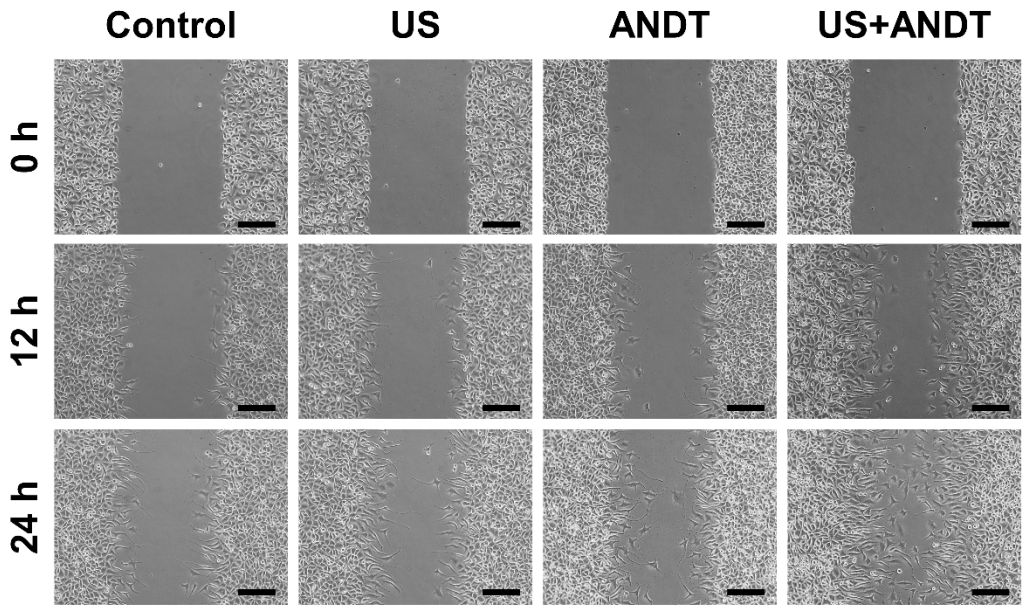

Fig. S9 Cell migration images of fibroblasts for 0, 12 and 24 h in control, US, ANDT, US+ANDT groups (scale bars = 100 μm).

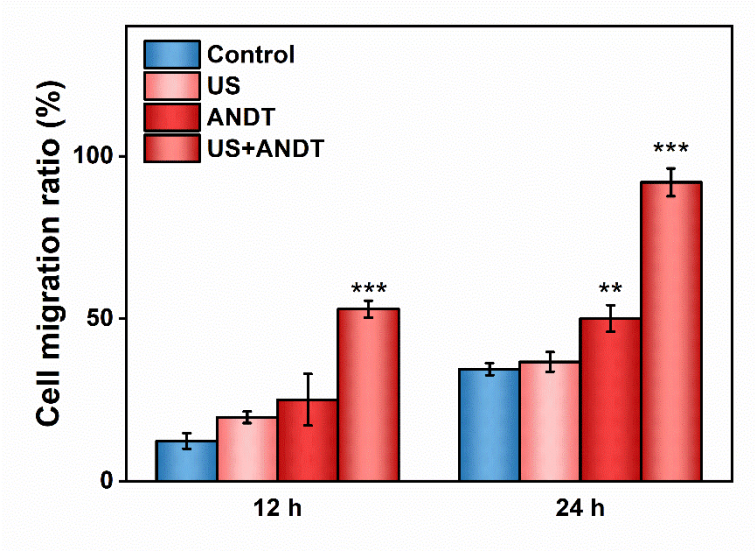

Fig.S10 Quantitative analysis of cell migration.

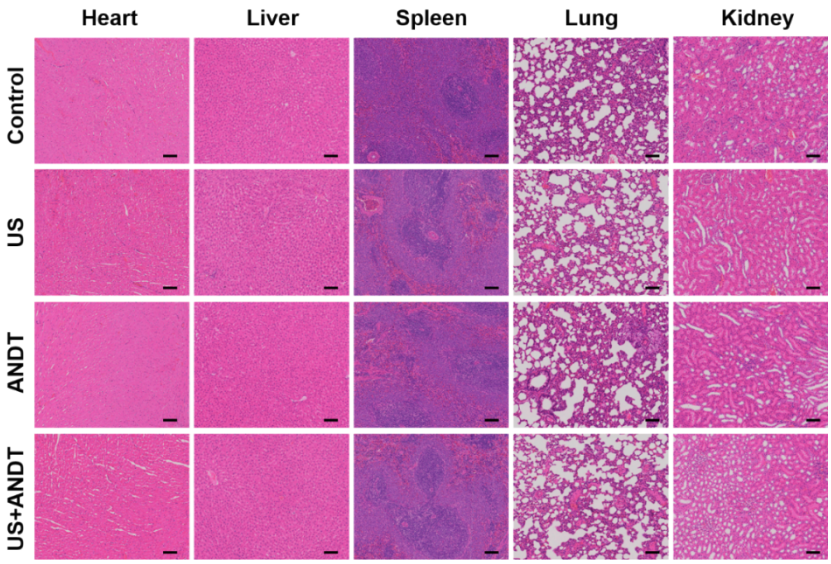

Fig. S11 HE staining of heart, liver, spleen, lung, and kidney in different groups (scale bars = 100 μm).

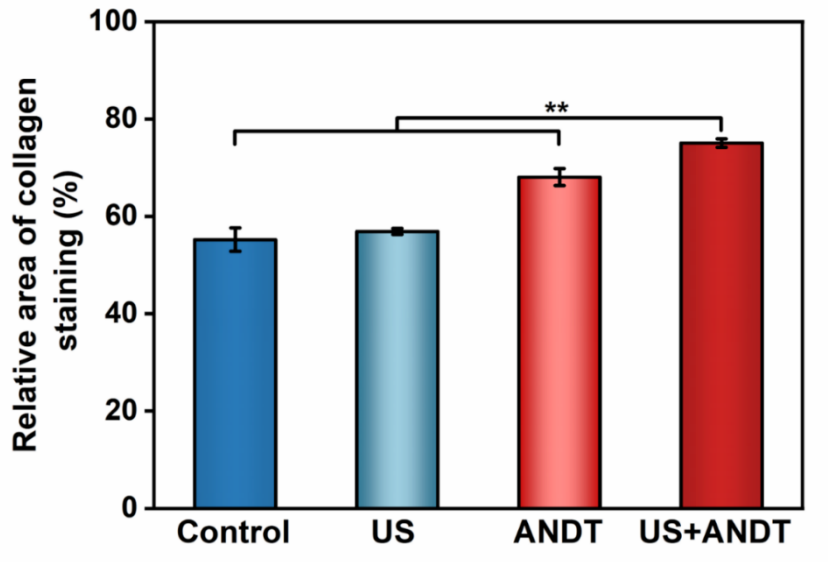

Fig. S12 Quantitative analysis of collagen density ($n = 3$, $^{**}p < 0.01$).